

Optical and submillimetre observations of Bok globules – tracing the magnetic field from low to high density

D. Ward-Thompson¹*, A. K. Sen², J. M. Kirk¹, D. Nutter¹

¹School of Physics and Astronomy, Cardiff University, Cardiff, CF24 3AA

²Department of Physics, Assam University, Silchar, 788 011, India

1 June 2009

ABSTRACT

We present optical and submillimetre polarimetry data of the Bok globule CB3. We also present optical polarimetry and submillimetre continuum data of the Bok globule CB246. We use each set of polarimetry data to infer the magnetic field orientation in each of the clouds. The optical data can only trace the field orientation in the low density edge regions of clouds, because if the extinction is too high then no optical emission is transmitted. The submillimetre data can only trace the field orientation in the high density central regions of the clouds, because current submillimetre polarimeters are only sensitive to high column densities.

It has previously been found that near-infrared polarisation mapping of background stars does not accurately trace the magnetic field in dense cloud regions, and hence that the grains responsible for near-infrared polarisation are under-represented in those regions. This may be due to a lack of aligned grains in dense regions. We test this by comparing the field orientations measured by our two independent methods of optical and submillimetre polarimetry. We find that the field orientation deduced from the optical data matches up well with the orientation estimated from the submillimetre data. We therefore claim that both methods are accurately tracing the same magnetic field in CB3. Hence, in this case, there must be significant numbers of aligned dust grains in the high density region, and they do indeed trace the magnetic field in the submillimetre.

We find an offset of 40 ± 14 degrees between the magnetic field orientation and the short axis of the globule. This is consistent with the mean value of 31 ± 3 degrees found in our previous work on prestellar cores, even though CB3 is a protostellar core. CB246 is a prestellar core, and in this case the offset between the magnetic field orientation inferred from the optical polarisation data and the short axis of the core inferred from the submillimetre continuum data is 28 ± 20 degrees. Taken together, the six prestellar cores that we have now studied in this way show a mean offset between magnetic field orientation and core short axis of $\sim 30 \pm 3$ degrees, in apparent contradiction with some models of magnetically dominated star formation.

Key words: stars: formation – ISM: clouds – ISM: dust, extinction – polarimetry

1 INTRODUCTION

Many models of star formation predict that magnetic fields play some role in the star formation process (Mestel & Spitzer 1956; Mouschovias 1976a,b; Nakano & Nakamura 1978; Ciolek & Mouschovias 1994; Ostriker, Gammie, & Stone 1999; Li & Nakamura 2004). However, measuring magnetic fields in space is notoriously difficult. Zeeman measurements allow one to measure the line-of-sight field strength using the line splitting of differ-

ent electronic magnetic moment states in the presence of a magnetic field (Zeeman 1897; Verschuur 1969; Crutcher 1999; Troland & Crutcher 2008). Faraday rotation of a background polarized source seen through a region containing a magnetic field can also be used to measure the line-of-sight field strength through that region (Burn 1966; Sokoloff et al. 1998).

The orientation of the magnetic field in the plane of the sky can be measured via the effects of aligned dust grains. The method of grain alignment has been a matter of debate for many years (e.g. Davis & Greenstein 1951; Jones & Spitzer 1967; Purcell 1979; Lazarian 1995a,b;

* e-mail: D.Ward-Thompson@astro.cf.ac.uk

Draine & Weingartner 1996). However, the various methods are generally lumped together under the name of the Davis-Greenstein effect (Davis & Greenstein 1951).

All methods predict that the grains align with their long axes perpendicular to the magnetic field. Hence in the optical and near-infrared, where the polarization is caused by preferential extinction by aligned elongated grains of a background unpolarized source (Hall 1949; Hiltner 1949), the polarization orientation is parallel to the field. In the far-infrared and submillimetre, where the polarization is caused by preferential emission from aligned elongated dust grains (Dennison 1977; Cudlip et al. 1982; Hildebrand, Dragovan, & Novak 1984), the polarization orientation is perpendicular to the field orientation (Dennison 1977).

The method of tracing the magnetic field using optical polarization of background starlight typically only works in regions of low extinction ($A_V \sim 1\text{--}5$). So this technique is mainly applicable towards the low-density edge regions of the clouds. This is because these data use preferential extinction of background starlight by aligned grains to produce the polarization. At higher extinctions the background starlight tends to be completely extinguished and it is not possible to measure any polarization (e.g. Vrba, Strom, & Strom 1976; Wilking et al. 1979)

The method of tracing the magnetic field using submillimetre polarization by preferential emission can typically only be measured in regions of high extinction – $A_V \sim 10\text{--}100$ (e.g., Ward-Thompson et al. 2000; Matthews, Wilson, & Fiege 2001; Kirk, Ward-Thompson, & Crutcher 2006). Hence the submillimetre data can only trace the field orientation towards the high density central regions of the clouds. This is because these data use preferential emission from aligned dust grains to produce the polarization, and are only sensitive to very high column densities in cloud centres.

At lower column densities, submillimetre polarimeters do not currently have the sensitivity to detect polarized emission. Furthermore, the nature of the usual data-taking method, using a chopping secondary mirror, ensures that any spatially extended components associated with the outer parts of the cloud are chopped away. Consequently, a combination of these two methods, of optical and submillimetre polarimetry, in theory provides a way of tracing the magnetic field from the low extinction outer parts of molecular clouds, to the high extinction, compact, central, dense parts of clouds.

It has previously been found (Goodman et al. 1995) that near-infrared polarization mapping of background stars does not accurately trace the magnetic field in dense cloud regions. This is based on the observation that near-infrared polarization levels, caused by preferential extinction by aligned grains, do not appear to rise sufficiently in denser cloud regions (Goodman et al. 1995).

This is not an effect of extinction preventing the infrared emission from escaping the cloud. Instead, these authors concluded that the grains responsible for polarising background starlight are under-represented in dense cloud regions (Goodman et al. 1995). There are two possible explanations for this: either there is a lack of aligned grains in dense regions; or that only a small fraction of the dust grain

size population in dense regions lies in the correct size range to polarise near-infrared emission from background stars.

In this paper we attempt to test the first of these hypotheses, whether or not there are significant numbers of aligned grains in high density regions. We do this by comparing submillimetre polarization measurements in high-density regions with optical polarization measurements in lower-density regions of the same cloud for a case in which both sets of measurements have been taken.

The submillimetre data cannot be affected by lower density foreground, or extended, field components, since they are not sensitive to these components. If the submillimetre and optical polarisations agree, then it would be difficult to avoid the conclusion that the magnetic field is continuous from low to high density and that the dust grains in the high-density regions are tracing the magnetic field in those regions. This would lead to the conclusion that there are significant numbers of aligned grains in the high-density regions.

2 OBSERVATIONS

Optical polarization measurements were made at the 1.2-metre telescope at Gurushikhar, Mount Abu, India, at latitude = $+24^\circ 36'$, longitude = $+72^\circ 43'$ (Sen et al. 2000). The Cassegrain focal station was used, giving an $f/13$ focus. The instrument used was the Imaging Polarimeter, IMPOL, of the Inter University Centre for Astronomy and Astrophysics (IUCAA), Pune, India. A description of the instrument is given by Sen & Tandon (1994) and Ramaprakash et al. (1998).

The design of the IMPOL polarimeter was based on the Durham Polarimeter (Scarrott et al. 1983; Ward-Thompson et al. 1985). It uses a Wollaston prism and half-wave plate to observe two orthogonal polarization states simultaneously. This removes the effects of sky polarization. A CCD camera was used to image the data. A broad-band white light filter was used, which corresponds to the wavelength range $0.45\text{--}0.7 \mu\text{m}$. The observations were carried out with typically a 500-sec exposure time for each object. The polarimetric data reduction procedure is described in detail by Sen et al. (2000).

We here report on optical polarization data of Bok globules CB3 and CB246, from the catalogue of Clemens & Barvainis (1988). These data were first published by Sen et al. (2000) as part of a larger study. The data were taken on 1997 December 23–25. The polarization was measured of stars background to the clouds and seen through the cloud periphery. The stars are generally of visual magnitude 12 or fainter.

Maps of the optical polarization vectors for these globules were mostly produced for the outer parts of the clouds, where the optical extinction was not so high. CB3 exhibited polarization values generally below 2%, whereas for CB246 it was a little higher. A detailed analysis of the nature of these polarization values was presented by Sen et al. (2005).

The submillimetre observations were made at the James Clerk Maxwell Telescope (JCMT), Mauna Kea, Hawaii, using the Submillimetre Common User Bolometer Array (SCUBA). SCUBA contained a pair of hexagonal, close-

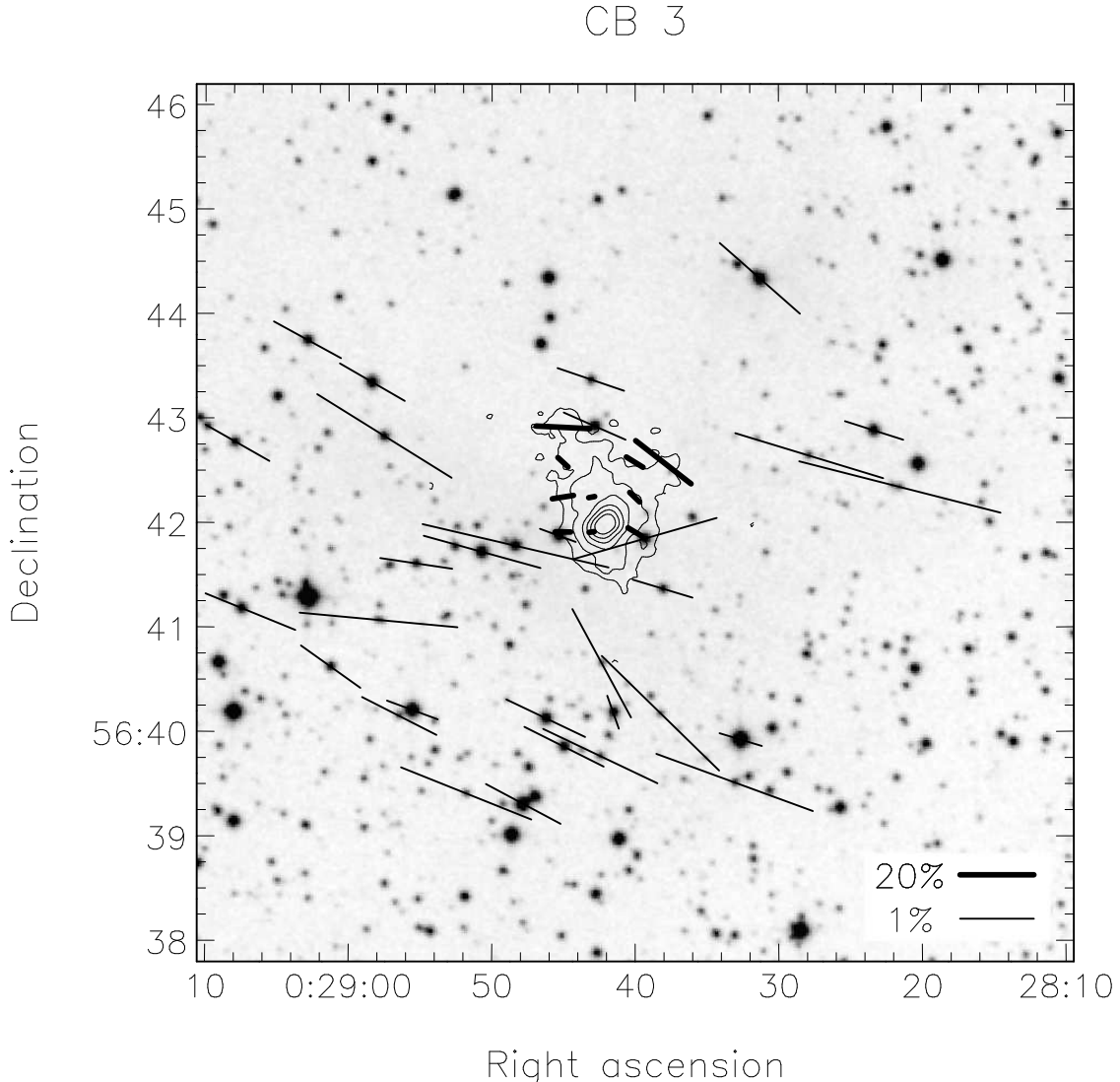


Figure 1. Polarization map of CB3. The thin vectors are the optical polarisation vectors from Sen et al. (2000). The thick vectors are the submm polarisation vectors from SCUBAPOL (Matthews et al. 2009), which have been rotated through 90 degrees to illustrate the magnetic field orientation in the same manner as the optical polarisation vectors (see text for discussion). The underlying greyscale image is the optical image of the region, taken from the digitized sky survey (Lasker 1994), obtained using the SkyView interface (McGlynn & Scollick 1994). The contours are isophotal contours of 850- μ m continuum emission as mapped by SCUBA. Note the good agreement between the field orientations inferred independently from the optical and submm polarisation data.

packed, bolometer arrays that could take data at 850 and 450 microns simultaneously, using a dichroic beam-splitter (Holland et al. 1999). SCUBA polarisation measurements were taken with the SCUBA polarimeter, SCUBAPOL (Greaves et al. 2003), which used a rotating half-waveplate and fixed analyser.

The waveplate was stepped through 16 positions (each offset from the last by 22.5°) and a Nyquist-sampled image (using a 16-point jiggle pattern) was taken at each waveplate position (Holland et al. 1996; Greaves et al. 2003). The observations were carried out whilst chopping the secondary mirror 120 arcsec in azimuth at 7 Hz and synchronously detecting the signal, thus rejecting sky emission. The integration time per point in the jiggle cycle was 1 sec, in each of the left and right beams of the dual-beam telescope chop. The total on-source integration time per complete cy-

cle was 512 sec. Only 850-micron data have been used in this paper. The instrumental polarization (IP) was removed using the measured value of Greaves et al. (2003). This was $0.92 \pm 0.05\%$ at a position angle of 163 ± 2 degrees. This was measured on planets and found to be stable with time. The main cause of the IP was believed to be the telescope wind blind. SCUBA and SCUBAPOL suspended operations in 2006, pending the commissioning of the next generation SCUBA2 instrument.

Di Francesco et al. (2008) and Matthews et al. (2009) have released near-complete legacy datasets for SCUBA and SCUBAPOL respectively. The SCUBA polarisation data presented in this paper come from the Matthews et al. (2009) legacy data set. The data were originally taken on 1998 August 10. The Stokes I, Q & U maps were calculated by Matthews et al. (2009) by fitting a sinusoid to the inten-

No.	R.A. (2000)	Dec. (2000)	PA [°]
Submm			
–	00 ^h 28 ^m	45.1 ^s +56°	41' 55" 90±19
–	00 ^h 28 ^m	42.7 ^s +56°	41' 55" 98±14
–	00 ^h 28 ^m	40.3 ^s +56°	41' 55" 59±8
–	00 ^h 28 ^m	45.1 ^s +56°	42' 15" 99±12
–	00 ^h 28 ^m	42.7 ^s +56°	42' 15" 102±14
–	00 ^h 28 ^m	40.3 ^s +56°	42' 15" 46±18
–	00 ^h 28 ^m	45.1 ^s +56°	42' 35" 47±23
–	00 ^h 28 ^m	40.3 ^s +56°	42' 35" 58±15
–	00 ^h 28 ^m	37.8 ^s +56°	42' 35" 52±7
–	00 ^h 28 ^m	45.1 ^s +56°	42' 55" 87±9
Optical			
16	00 ^h 28 ^m	39.0 ^s +56°	41' 19" 73±6
19	00 ^h 28 ^m	49.0 ^s +56°	41' 45" 76±1
20	00 ^h 28 ^m	40.2 ^s +56°	41' 48" 106±1
21	00 ^h 28 ^m	46.1 ^s +56°	41' 50" 70±2
27	00 ^h 28 ^m	43.5 ^s +56°	42' 52" 66±1
29	00 ^h 28 ^m	43.7 ^s +56°	43' 18" 71±6

Table 1. Position angles of the magnetic field vectors shown in Figure 1 across CB3. The submm polarisation angles have been rotated by 90 degrees to indicate the orientation of the magnetic field, for direct comparison with the optical polarisation angles (see text for discussion).

sity measurements from the different waveplate angles. The Stokes maps were then converted by us into tabulated lists of polarisation vectors. We binned the I, Q & U maps to a resolution of 20 arcsec, and then calculated the polarisation vector at each pixel. Finally, a signal-to-noise ratio cut was applied to remove spurious vectors. The remaining vectors are plotted in Figure 1.

The continuum submillimetre data were taken separately from the polarisation data. For CB3 the data were downloaded from the SCUBA data archive while the data for CB246 were taken from Launhardt et al. (2009). The data were reduced in the usual manner (see, for example, Nutter & Ward-Thompson 2007) using the SURF software package (Jenness & Lightfoot 2000). The submillimetre zenith opacity for atmospheric extinction removal was determined by comparison with the 1.3-mm sky opacity (Archibald et al. 2002).

3 RESULTS

3.1 CB3

CB3 was catalogued by Clemens & Barvainis (1988), who noted it has an angular size of 6.7×5.6 arcmin. It is also known as Lynds 594 (Lynds 1962). It lies at an approximate distance of 2.5kpc (Launhardt & Henning 1997). It contains at least two young stellar objects (YSOs), one of which is a Class 0 source (Andre, Ward-Thompson, & Barsony 1993) driving a chemically active bipolar outflow (Codella & Bachiller 1999). Additionally there appear to be more than 20 very red K-band sources in the field clustered around the core (Launhardt et al. 1998). This cluster was compared to

the submillimetre emission by Huard, Weintraub, & Sandell (2000). CB3 is sometimes referred to as a site of intermediate mass star formation (Codella & Bachiller 1999; Klein et al. 2000). It is coincident with the IRAS source 00259+5625, which has a luminosity of $\sim 930 L_{\odot}$ (Codella & Bachiller 1999). There is also a water maser source associated with this globule (Scappini, Caselli, & Palumbo 1991).

Figure 1 shows the optical and submillimetre polarisation maps of CB3, superposed on a contour map of submillimetre continuum emission and a grey-scale image of optical continuum emission. The region of brightest submillimetre emission coincides with a blank area in the optical image, as expected for a dark dust cloud. Nevertheless, background stars are visible through the edge of the cloud. The optical and submillimetre polarisation vectors mostly appear to lie in a similar orientation.

We find the E(B-V) colours of the background stars to all lie in the range between 0.1 and 0.6 (Sen et al., in prep.). Taking the canonical ratio (Whittet et al., 2008, and references therein), we therefore estimate that these stars have $A_V \sim 0.3\text{--}1.8$. In the region covered by the outermost submillimetre contour, the mean column density is $\sim 10^{22} \text{ cm}^{-2}$ (Launhardt et al., 1997). This corresponds approximately to $A_V \sim 10$ (Frerking et al., 1982). This is precisely the level of extinction in which Goodman et al., (1995) found near-infrared polarisation levels lower than expected.

Table 1 lists the positions and position angles of the submillimetre vectors across CB3. The angles have been rotated by 90 degrees to show the orientation of the magnetic field. The mean and standard deviation of the position angle of the magnetic field derived from the Q and U values at each of the 10 positions is 69 ± 14 degrees.

Table 1 also lists the six optical magnetic field vectors which are closest to the submillimetre vectors – those optical vectors within an arcmin of the centre of the submillimetre emission. The mean and standard deviation of the position angle of these six optical vectors is 77 ± 15 degrees. Vector number 20 is seen to be significantly different from the other five vectors. This may be due to it being a foreground star. We note that it does have a lower than average value of E(B-V), consistent with this explanation (Sen et al., in prep.). If we exclude this vector and calculate the mean of the remainder, we obtain a mean of 72 ± 4 degrees.

Therefore, we see that the field orientation as estimated from the submillimetre polarisation is in very good agreement with that estimated from the optical polarisation. Consequently, we deduce that the magnetic field is continuous from the low to the high density regions, with a mean position angle of 71 ± 14 degrees. Furthermore, the dust grains in the high density region appear to be tracing the magnetic field well.

The submillimetre contours on Figure 1 show that this Bok globule is elongated. The same elongation is seen in various molecular line tracers of this core, such as CS (Codella & Bachiller 1999). We estimate that the position angle of the long axis of the globule is 21 ± 5 degrees. This is at an angle of 50 ± 14 degrees to the magnetic field orientation. Models of magnetically dominated star formation predict that the magnetic field should lie along the short axis of the star-forming core (e.g. Ciolek & Mouschovias 1994, 1998; Li & Shu 1996). In this case we see an offset of 40 ± 14 degrees from the short axis. This is similar to results we have

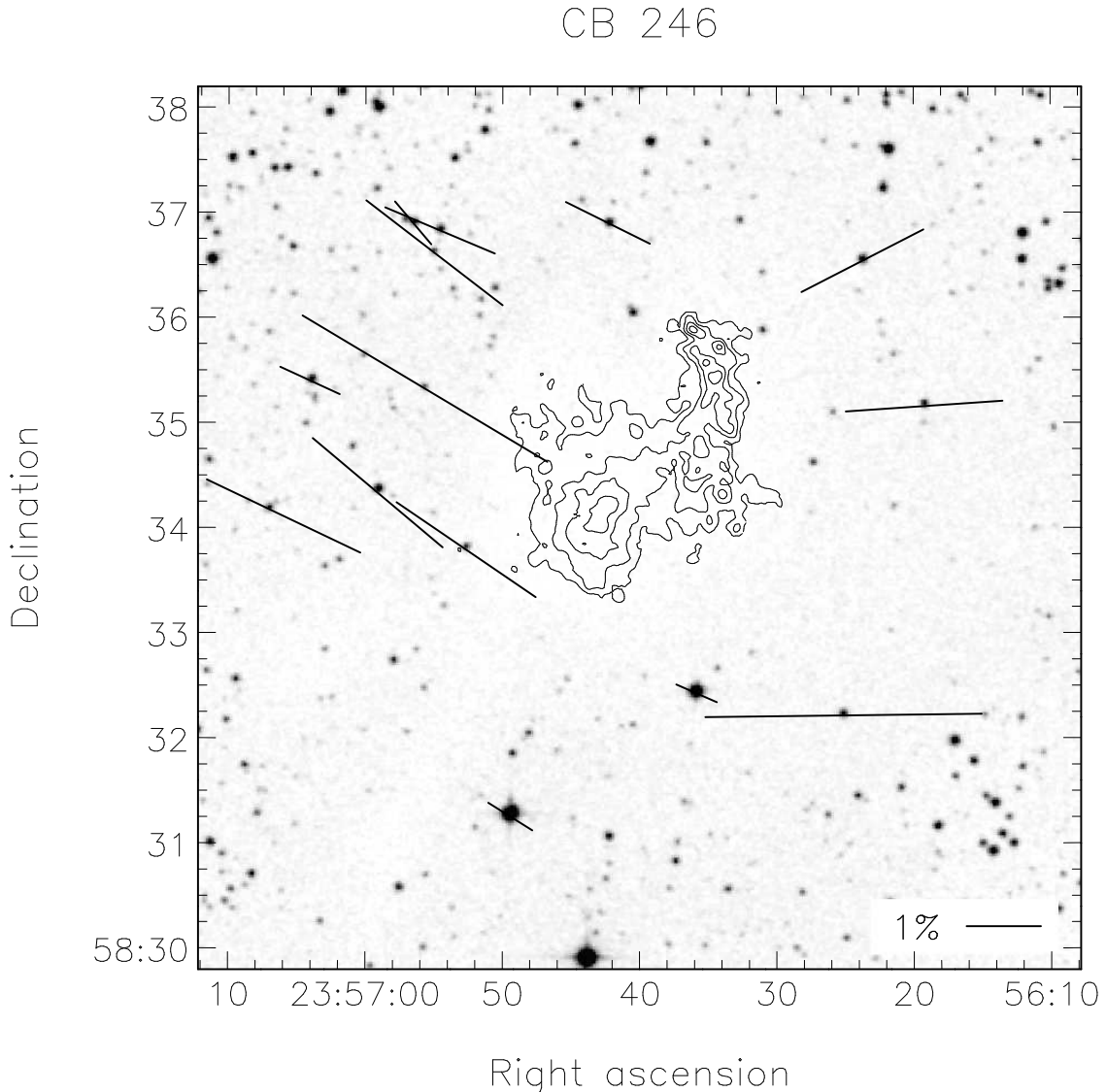


Figure 2. Polarization map of CB246. Details as in Figure 1. No submm polarisation data were available for this region. However, note how the field orientation inferred from the optical polarisation data lie offset from the short axis of the submm continuum emission from the core. Note also how both core and field appear to twist (see text for discussion).

seen previously in prestellar cores (Ward-Thompson et al. 2000; Kirk, Ward-Thompson, & Crutcher 2006). We return to this in section 4 below.

3.2 CB246

CB246 was catalogued by Clemens & Barvainis (1988), who noted it has an angular size of 7.8×4.5 arcmin. It is also known as Lynds 1253 (Lynds 1962). It lies at an approximate distance of 140pc (Launhardt & Henning 1997). It is a starless core, possibly prestellar in nature (Ward-Thompson et al. 2007). Scappini & Codella (1996) list this source as inactive, with neither a water maser nor molecular outflow. However, their detection of NH₃ and C₂S made them postulate that the source was more advanced than the other sources in their survey. They followed up their survey with a targeted observation

(Codella & Scappini 1998), which confirmed their earlier findings. Lee, Myers, & Tafalla (2001) classified CB246 as having significant red excess, but no blue asymmetry in the CS spectra, indicating that the core has not begun to collapse.

Figure 2 shows the optical polarisation map of CB246, superposed on a contour map of submillimetre continuum emission and a grey-scale image of optical continuum emission. The region of brightest submillimetre emission coincides with a blank area in the optical image, as expected for a dark dust cloud. Nevertheless, background stars are visible through the edge of the cloud. No submillimetre polarimetry data were available for this cloud, but we can infer the plane-of-sky magnetic field orientation from the optical polarisation vectors.

We note that the vectors to the east of the core centre have a systematically different mean position angle from those to the west. Similarly the core long axis orientation

Core	Offset
L1544	29 ± 6
L183	34 ± 6
L43	44 ± 6
L1498	19 ± 12
L1517B	25 ± 6
CB3	40 ± 14
CB246	28 ± 20

Table 2. Position angle offsets between the magnetic field orientation and the short axis of the core for the five prestellar cores previously measured, together with the two sources studied in the current work (see text for discussion).

also appears to shift from east to west. Therefore, we compare the mean position angles of the magnetic field and core long axis separately in the eastern and western parts of the core. In the east, the plane-of-sky magnetic field lies at a position angle of 60 ± 3 degrees. The long axis of the core in the east appears to lie along a position angle of roughly 122 ± 5 degrees. Hence the short axis is at position angle 32 ± 5 degrees. The approximate angular offset between the magnetic field and the short axis of the globule is therefore 28 ± 8 degrees for the eastern half of the core.

In the west, the plane-of-sky magnetic field lies at a position angle of 94 ± 5 degrees. The long axis of the core in the west appears to lie along a position angle of roughly 157 ± 5 degrees. Hence the short axis is at position angle 67 ± 5 degrees. The approximate angular offset between the magnetic field and the short axis of the globule is therefore 27 ± 10 degrees for the western half of the core.

The weighted mean of these two offsets is therefore 28 degrees. The mathematical error-bar on this value is less than 10 degrees. However, given that the core and field both curve by more than 30 degrees we do not claim an error-bar of less than 20 degrees for this estimate, as this is the error-bar obtained if one treats the whole core simultaneously. A detailed submillimetre polarisation map of CB246 could potentially confirm that the curvature of the field exactly mirrors the curvature of the core throughout its length. In that case a smaller error-bar could be ascribed to the offset value. Nevertheless, the value of 28 degrees is still consistent with prestellar cores we have observed previously (see next section).

4 DISCUSSION

The fact that we have observed a consistent magnetic field orientation in CB3 for both the optical and submillimetre polarisation data shows that both are tracing the same magnetic field. This implies that dust grains in the high-density regions of this globule are indeed tracing the magnetic field. Hence, there must be significant numbers of aligned grains in the high-density regions. Furthermore, the magnetic fields must be continuous from low to high density. Therefore, the previous finding (Goodman et al. 1995), that dust grains in high-density regions do not trace the magnetic field in near-infrared polarisation measurements, cannot be explained by a lack of aligned grains. Our findings are consistent with those of Whittet et al. (2008), who conclude from their data

that there is no change in grain alignment efficiency from low- to high-density regions of dust clouds.

In addition, these data allow us to comment on the influence of magnetic fields on the star formation process. Magnetically-dominated models of star formation predict that a cloud should collapse first along the magnetic field lines, and then subsequently contract quasi-statically perpendicular to the field orientation (e.g. Ciolek & Mouschovias 1994). Hence these models predict that the magnetic field should lie along the short axis of a collapsing cloud core.

Ward-Thompson et al. (2000) presented the first observations of the magnetic field geometry in pre-stellar cores when they mapped L183, L1544 and L43 with the SCUBA polarimeter. Their maps showed relatively smooth and uniform magnetic fields over the central core regions. However, in each case they observed an offset between the short axis of the core and the magnetic field orientation. Kirk, Ward-Thompson, & Crutcher (2006) studied the prestellar cores L1498 and L1517B in a similar manner and also observed similar offsets. An attempt to explain these offsets in terms of tri-axial cores viewed from arbitrary angles was proposed by Basu (2000), but no magnetic model incorporating this additional complication has been put forward.

Table 2 lists the cores observed previously, together with those from this work, and the offset observed in each case between the magnetic field orientation and the short axis of the core. The weighted mean offset of the five previously observed cores is 31 ± 3 degrees. We note that the two globules observed in the current study both have offsets consistent with this value. This is in spite of the fact that CB3 is not a starless core, but a protostellar core. CB246 is a starless core. The weighted mean of the six starless cores in Table 2 is $\sim 30 \pm 3$ degrees. This appears to be in contradiction with some models of magnetically moderated star formation.

5 CONCLUSIONS

We have used optical and submillimetre polarimetry of Bok globule CB3 to infer the magnetic field orientation. The optical data trace the field orientation in low density regions and the submillimetre data trace the field orientation in high density regions. We have tested a hypothesis that there is a lack of aligned dust grains in high density regions, causing near-infrared polarisation levels to be lower than expected, by comparing the field orientations measured by our two independent methods.

We found that the field orientation deduced from the optical polarization data matches up well with the orientation estimated from the submillimetre measurements. The inferred field lines join up from low to high extinction and produce a consistent and coherent picture of the whole magnetic field in CB3. We saw that both methods accurately trace the same magnetic field. Hence we deduce that there are significant numbers of aligned grains in the high-density regions of CB3. Furthermore, these aligned dust grains appear to trace the magnetic fields in those regions, as mapped in submillimetre polarisation.

We have also compared polarisation data with submillimetre continuum data in Bok globules CB3 and CB246. We have compared the field orientations with the core mor-

photologies and found an offset in each case between the field orientation and the short axis of the globule. These offsets are consistent with those seen in previous studies of prestellar cores, despite the fact that, of our two globules, only CB246 is a starless core. Taken together, the six starless cores that we have now studied in this way are beginning to show a consistent picture of an offset between magnetic field orientation and core short axis of $\sim 30 \pm 3$ degrees, in apparent contradiction with some models of magnetically dominated star formation.

ACKNOWLEDGEMENTS

JMK and DJN acknowledge the UK STFC for PDRA support through the Cardiff Astronomy Rolling Grant. The JCMT is operated by the Joint Astronomy Centre, Hawaii, on behalf of the UK STFC, the Netherlands NWO, and the Canadian NRC. The 1.2-metre telescope at Mount Abu is operated by the Physical Research Laboratory of India. This research used the facilities of the Canadian Astronomy Data Centre, operated by the National Research Council of Canada, with the support of the Canadian Space Agency. The Digitized Sky Survey was produced at the Space Telescope Science Institute under U.S. Government grant NAG W-2166. The images of these surveys are based on photographic data obtained using the Oschin Schmidt Telescope on Palomar Mountain and the UK Schmidt Telescope at Siding Spring. The plates were processed into the present compressed digital form at the Royal Observatory Edinburgh (ROE) photolabs, with the permission of these institutions. The authors also acknowledge the use of NASA's SkyView facility (<http://skyview.gsfc.nasa.gov>).

REFERENCES

- Andre P., Ward-Thompson D., Barsony M., 1993, ApJ, 406, 122
 Archibald E. N., et al., 2002, MNRAS, 336, 1
 Basu S., 2000, ApJ, 540, L103
 Burn B. J., 1966, MNRAS, 133, 67
 Ciolek G. E., Mouschovias T. C., 1994, ApJ, 425, 142
 Ciolek G. E., Mouschovias T. C., 1998, ApJ, 504, 280
 Clemens D. P., Barvainis R., 1988, ApJS, 68, 257
 Codella C., Bachiller R., 1999, A&A, 350, 659
 Codella C., Scappini F., 1998, MNRAS, 298, 1092
 Crutcher R. M., 1999, ApJ, 520, 706
 Cudlip W., Furniss I., King K. J., Jennings R. E., 1982, MNRAS, 200, 1169
 Davis L. J., Greenstein J. L., 1951, ApJ, 114, 206
 Dennison B., 1977, ApJ, 215, 529
 Di Francesco J., Johnstone D., Kirk H., MacKenzie T., Ledwosinska E., 2008, ApJS, 175, 277
 Draine B. T., Weingartner J. C., 1996, ApJ, 470, 551
 Goodman A. A., Jones T. J., Lada E. A., Myers P. C., 1995, ApJ, 448, 748
 Greaves J. S., et al., 2003, MNRAS, 340, 353
 Hall J. S., 1949, Sci, 109, 166
 Hildebrand R. H., Dragovan M., Novak G., 1984, ApJ, 284, L51
 Hiltner W. A., 1949, Sci, 109, 165
 Huard T. L., Weintraub D. A., Sandell G., 2000, A&A, 362, 635
 Holland W. S., Greaves J. S., Ward-Thompson D., André P., 1996, A&A, 309, 267
 Holland W. S., et al., 1999, MNRAS, 303, 659
 Jenness T., Lightfoot J.F., 2000, Starlink User Note 216, Starlink Project, CCLRC
 Jones R. V., Spitzer L. J., 1967, ApJ, 147, 943
 Kirk J. M., Ward-Thompson D., Crutcher R. M., 2006, MNRAS, 369, 1445
 Klein R., Henning T., Launhardt R., Feldt M., 2000, AGM, 17, 6
 Lasker B. M., 1994, IAUS, 161, 167
 Launhardt R., Evans N. J., II, Wang Y., Clemens D. P., Henning T., Yun J. L., 1998, ApJS, 119, 59
 Launhardt R., Ward-Thompson D., Henning T., 1997, MNRAS, 288, 45
 Launhardt R., Nutter D., Ward-Thompson D., Khanzadyan T., Bourke T. L., Wolf S., Henning Th., Zylka R., A&A, in prep.
 Launhardt R., Henning T., 1997, A&A, 326, 329
 Lazarian A., 1995a, ApJ, 451, 660
 Lazarian A., 1995b, MNRAS, 277, 1235
 Lee C. W., Myers P. C., Tafalla M., 2001, ApJS, 136, 703
 Li Z.-Y., Nakamura F., 2004, ApJ, 609, L83
 Li Z.-Y., Shu F. H., 1996, ApJ, 472, 211
 Lynds B. T., 1962, ApJS, 7, 1
 Matthews B. C., Wilson C. D., Fiege J. D., 2001, ApJ, 562, 400
 Matthews B., McPhee C., Fissel L., Curran R., ApJS, 2009, in press
 McGlynn T., Scollick K., 1994, ASPC, 61, 34
 Mestel L., Spitzer L., Jr., 1956, MNRAS, 116, 503
 Mouschovias T. C., 1976a, ApJ, 206, 753
 Mouschovias T. C., 1976b, ApJ, 207, 141
 Nakano T., Nakamura T., 1978, PASJ, 30, 671
 Nutter D., Ward-Thompson D., 2007, MNRAS, 374, 1413
 Ostriker E. C., Gammie C. F., Stone J. M., 1999, ApJ, 513, 259
 Purcell E. M., 1979, ApJ, 231, 404
 Ramaprakash A. N., Gupta R., Sen A. K., Tandon S. N., 1998, A&AS, 128, 369
 Scappini F., Codella C., 1996, MNRAS, 282, 587
 Scappini F., Caselli P., Palumbo G. G. C., 1991, MNRAS, 249, 763
 Scarrott S. M., Warren-Smith R. F., Pallister W. S., Axon D. J., Bingham R. G., 1983, MNRAS, 204, 1163
 Sen A. K., Tandon S. N., 1994, SPIE, 2198, 264
 Sen A. K., Gupta R., Ramaprakash A. N., Tandon S. N., 2000, A&AS, 141, 175
 Sen A. K., Mukai T., Gupta R., Das H. S., 2005, MNRAS, 361, 177
 Sokoloff D. D., Bykov A. A., Shukurov A., Berkhuijsen E. M., Beck R., Poezd A. D., 1998, MNRAS, 299, 189
 Troland T. H., Crutcher R. M., 2008, ApJ, 680, 457
 Verschuur G. L., 1969, ApJ, 156, 861
 Vrba F. J., Strom S. E., Strom K. M., 1976, AJ, 81, 958
 Ward-Thompson D., Warren-Smith R. F., Scarrott S. M., Wolstencroft R. D., 1985, MNRAS, 215, 537
 Ward-Thompson D., Kirk J. M., Crutcher R. M., Greaves J. S., Holland W. S., André P., 2000, ApJ, 537, L135

- Ward-Thompson D., André P., Crutcher R., Johnstone D., Onishi T., Wilson C., 2007, Protostars and Planets V, 33 Whittet D. C. B., Hough J. H., Lazarian A., Hoang T., 2008, ApJ, 674, 304 Wilking B. A., Lebofsky M. J., Kemp J. C., Rieke G. H., 1979, AJ, 84, 199 Zeeman P., 1897, ApJ, 5, 332